Exhibit B

nature medicine

The RAB25 small GTPase determines aggressiveness of ovarian and breast cancers

Kwai Wa Cheng[1], John P Lahad[1], Wen-lin Kuo[2], Anna Lapuk[2], Kyosuke Yamada[2], Nelly Auersperg[3], Jinsong Liu[4], Karen Smith-McCune[5], Karen H Lu[6], David Fishman[7], Joe W Gray[2] & Gordon B Mills[1]

High-density array comparative genomic hybridization (CGH)[1] showed amplification of chromosome 1q22 centered on the *RAB25* small GTPase[2], which is implicated in apical vesicle trafficking[3], in approximately half of ovarian and breast cancers. *RAB25* mRNA levels were selectively increased in stage III and IV serous epithelial ovarian cancers compared to other genes within the amplified region, implicating *RAB25* as a driving event in the development of the amplicon. Increased DNA copy number or RNA level of *RAB25* was associated with markedly decreased disease-free survival or overall survival in ovarian and breast cancers, respectively. Forced expression of *RAB25* markedly increased anchorage-dependent and anchorage-independent cell proliferation, prevented apoptosis and anoikis, including that induced by chemotherapy, and increased aggressiveness of cancer cells *in vivo*. The inhibition of apoptosis was associated with a decrease in expression of the proapoptotic molecules, BAK and BAX, and activation of the antiapoptotic phosphatidylinositol 3 kinase (PI3K) and AKT pathway, providing potential mechanisms for the effects of *RAB25* on tumor aggressiveness. Overall, these studies implicate *RAB25*, and thus the RAB family of small G proteins, in aggressiveness of epithelial cancers.

Ovarian cancer remains the fifth most frequent cause of cancer death in women. An improved understanding of the genetic aberrations in ovarian cancer may identify new etiologic, prognostic or therapeutic targets that can improve patient management. Several genes located at sites of DNA copy number aberrations in ovarian cancer, including *PIK3CA*[4], *ERBB2* (ref. 5), *MYC*[6], *EEF1A2* (ref. 7), *AKT2* (ref. 8) and *NCOA3* (ref. 9), have been implicated in the pathophysiology of ovarian cancer. Importantly, chromosome CGH analyses reveal other regions of recurrent abnormality in ovarian cancer, which may encode additional genes contributing to tumor behavior[10–12]. In particular, chromosome 1q is frequently increased in copy number in ovarian[11,12] and breast[13] cancers and Wilms[14] tumors; a high relapse rate in invasive ductal breast carcinomas[13] and Wilms tumors[14] are associated with increased DNA copy number on chromosome 1q, but the driver of the regional copy number increase at 1q has not been identified.

Using array CGH[1] to more precisely define region(s) of recurrent copy number increase on chromosome 1q, we delineated an increase (at least 1.3-fold) in DNA copy number in a 1.1-Mb region located on chromosome 1q22 in 28 of 52 (54%) of advanced serous epithelial ovarian cancers (Fig. 1a). Notably, ovarian cancer patients with elevated 1q22 (at least 1.5 copies of *RAB25*) either did not enter a disease-free state following surgery and chemotherapy or showed very short disease-free survival, implicating gene(s) in this region as potential oncogenes regulating the behavior of ovarian cancers (Fig. 1b).

The minimal region of copy number increase on 1q22 encompassed the region from position 152,377,895 to 153,495,551, which contains a total of 34 genes, including 22 known genes and 12 hypothetical proteins based on the July 2003 human reference sequence. Based on expression levels from our microarray data sets[15], the Gene Expression Omnibus and the Stanford Microarray Database, we eliminated 18 candidates that did not show a significant difference in RNA levels between normal ovarian epithelium (NOE) and ovarian cancers. We analyzed mRNA expression levels of the remaining 16 open reading frames located in this region using real-time quantitative PCR to identify potential drivers of the copy number increase at 1q22. Although mRNA levels of several of the genes in this region were modestly elevated in a fraction of ovarian cancers as compared to NOE or benign ovarian tumors, *RAB25* mRNA levels were markedly increased in 55 of 62 (88.7%) of ovarian cancers ($P < 0.001$; Fig. 1c,d). This observation was confirmed in an independent ovarian cancer data set[16] wherein *RAB25* transcript levels were increased in 35 of 44 (80%) ovarian cancer samples compared to NOE. The increase in *RAB25* expression was stage dependent, with stage III and stage IV cancers showing higher levels ($P < 0.01$; Fig. 1d) than early stage cancers, suggesting a potential role of *RAB25* in tumor progression. Sequencing of the open reading frame in 8 ovarian cancer samples did not identify mutations in *RAB25*, suggesting that mutation of *RAB25* rarely or never occurs in ovarian cancer. Linear regression analysis of 21 epithelial ovarian cancers for which both CGH and expression levels were available showed a direct relationship between copy number and expression of *RAB25* (Fig. 1e) with

[1]Department of Molecular Therapeutics, University of Texas MD Anderson Cancer Center, Houston, Texas 77054, USA. [2]Lawrence Berkley National Laboratory, Berkeley, California 94720, USA. [3]Department of Obstetrics and Gynecology, University of British Columbia, Vancouver, British Columbia V6H 3V5, Canada. [4]Department of Pathology, [6]Department of Gynecological Oncology, University of Texas MD Anderson Cancer Center, Houston, Texas, 77030, USA. [5]Department of Obstetrics and Gynecology, University of California, San Francisco, San Francisco, California 94143, USA. [7]Department of Obstetrics and Gynecology, School of Medicine, New York University, New York, New York 10016, USA. Correspondence should be addressed to G.B.M. (gmills@mdanderson.org).

Published online 24 October 2004; doi:10.1038/nm1125

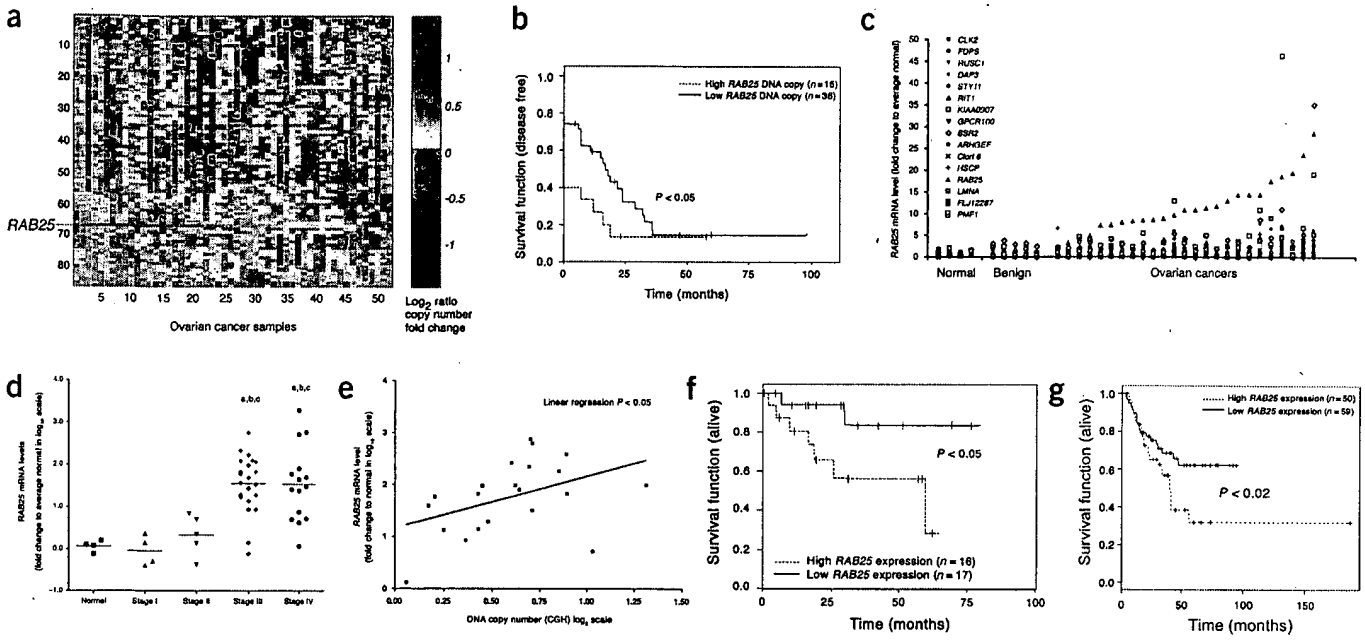

Figure 1 Genetic aberrations at chromosome 1q22. (a) Array CGH of chromosome 1 in ovarian cancer ordered by *RAB25*, with red and blue indicating increase and decrease in DNA copy number, respectively. (b) Disease-free survival in ovarian cancer patients with high *RAB25* DNA copy (at least 1.75-fold increase). (c) Real-time quantitative PCR of candidate genes from centromere to telomere in ovarian cancer. (d) Stage dependence of *RAB25* mRNA expression in ovarian cancer (a, $P < 0.001$ versus normal; b, $P < 0.001$ versus Stage I; c, $P < 0.01$ versus Stage II). (e) Correlation of *RAB25* DNA copy number and mRNA levels in ovarian cancer. (f,g) *RAB25* RNA levels on survival of ovarian cancer (f) and of breast cancer (g). Unless otherwise designated, ovarian cancers are epithelial serous Stage III–IV.

a Pearson coefficient value of 0.434 ($P < 0.05$) and a Spearman rank coefficient of 0.481 ($P < 0.05$). Of 53 patients with high *RAB25* mRNA (at least twofold increase) for which follow up data was available, 30 did not enter a disease-free interval (data not shown). As expected from CGH analysis (Fig. 1b), high *RAB25* mRNA expression (at least 40-fold increase compared to NOE, $P < 0.05$), assessed by real-time quantiative PCR and microarray[15], was associated with decreased survival (Fig. 1f) when comparing the top and bottom 30% of patients. When all patient samples ($n = 53$) were taken into consideration, a similar trend of correlation between high *RAB25* levels and outcome was observed (see Supplementary Fig. 1 online).

CGH analysis also indicated an increase (at least 1.3-fold) at 1q22 in the region of *RAB25* in 47% of breast cancers (JWG, unpublished data). In contrast to ovarian cancer, the regional increase in breast cancer is wide and encompasses the majority of 1q. Using an independent breast cancer microarray data set[17], 78 of 116 (66.7%) breast cancer patients showed an at least 1.7-fold increase in *RAB25* expression compared to normal breast tissue. Kaplan-Meier analysis of 109 breast cancer patients showed a correlation between high *RAB25* expression ($n = 50$; at least twofold higher than normal) and a decrease in both overall survival ($P < 0.02$, Fig. 1g) and disease-free survival ($P < 0.01$, Supplementary Fig. 2 online). *RAB25* levels were an independent indicator of disease-free interval and overall survival in breast cancer when the data were adjusted for tumor size, ER status and grade and stratified by metastases. Increased *RAB25* levels have previously been noted in prostate cancer[18], transitional cell carcinoma of the bladder[19] and invasive breast cancer[20], suggesting a pathological role for RAB25 in epithelial tumor development.

We evaluated the role of *RAB25* in the aggressiveness of ovarian and breast cancers by altering *RAB25* levels. Transient expression of *RAB25* in A2780, DOV13, HEY and OCC1 ovarian cancer cells markedly increased colony-forming activity under anchorage-dependent conditions (Fig. 2a). We thus established multiple breast and ovarian cancer cell lines that stably express *RAB25*. Stable expression of *RAB25* in ovarian T80 (SV-40– and telomerase-immortalized but nontumorigenic ovarian cancer cells[21]), A2780, OCC1, SKOV3 and HEY and breast MCF-7 cancer cells increased cell numbers under both low (1% fetal bovine serum (FBS)) and high (10% FBS) serum conditions (Table 1, Supplementary Fig. 3 online). The ability of *RAB25* to increase cell number could result from either increased cell-cycle progression or reduced apoptosis. Our analyses did not detect a significant change in cell-cycle progression as assessed by propidium iodide staining; however, enforced expression of *RAB25* in immortalized ovarian cancer cells T80 and T29 (Fig. 2b), A2780 (Fig. 2b) and HEY (data not shown) was sufficient to increase cell survival under multiple stress conditions including serum starvation, anoikis (anchorage-independent stress), UV radiation and paclitaxel, suggesting that *RAB25* regulates cell survival. To verify the role of *RAB25* in regulating cell survival, we employed RNA interference (RNAi)[22] technology to knock down the expression of *RAB25*. RNAi transfection markedly decreased both *RAB25* mRNA levels (Fig. 2c) and protein levels (Fig. 2c). Decreasing *RAB25* levels consistently increased the number of apoptotic cells in control (no UV radiation) and UV-irradiated breast and ovarian cancer cells (Fig. 2d), confirming a role for *RAB25* in regulating cellular apoptosis. Similarly, RNAi transfection also resulted in a significant ($P < 0.05$) decrease in cell proliferation (Supplementary Fig. 4 online), further confirming the role of *RAB25* in regulating cell survival.

Genes in the *BCL2* (B-cell lymphocyte/leukemia-2 gene) family[23], such as *BAK1* (Bcl-2 homologous antagonist/killer) and *BAX* (Bcl-2 associated protein x), have been shown to be central and key effectors of the mammalian apoptotic signaling cascade[24] and to regulate tumorigenesis[25]. Enforced *RAB25* expression decreased protein levels of BAK in A2780 and T29, whereas both BAX and BAK were

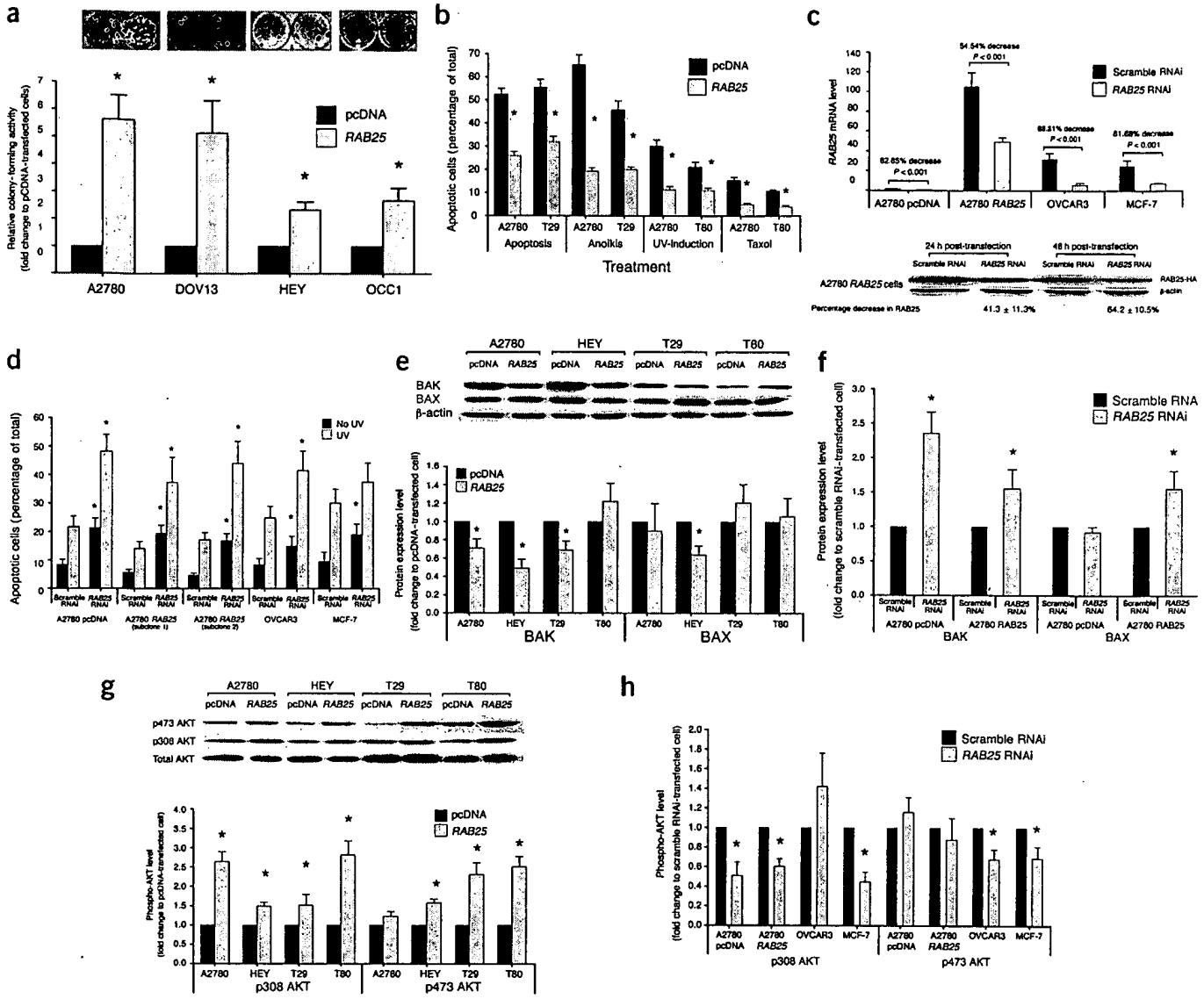

Figure 2 *RAB25* regulates cell proliferation and survival. (**a**) Effect of transient transfection of *RAB25* on colony formation. (**b**) Effect of stable expression of *RAB25* on apoptotic stress. *RAB25* siRNA decreases (**c**) *RAB25* mRNA (upper panel, measured as fold change to A2780 pcDNA scramble RNAi–transfected cells) and protein (lower panel) levels and (**d**) UV radiation–induced apoptosis. (**e**,**f**) Effect of *RAB25* stable expression (**e**) and *RAB25* RNAi (**f**) on BAK and BAX levels. (**g**,**h**) Effect of *RAB25* stable expression (**g**) and RNAi (**h**) on AKT phosphorylation. All results are mean ± s.d. of three individual experiments except colony formation, which is mean ± s.d. of triplicates in a representative experiment of three performed. At least two subclones of each line were assessed in each assay.

decreased in HEY ovarian cancer cells (Fig. 2e). Neither BAX nor BAK was decreased in T80, suggesting that mechanisms other than changes in BAX or BAK protein levels must also contribute to resistance to apoptosis in some cells. Nevertheless, downregulation of *RAB25* expression by RNAi reversed the RAB25-mediated inhibition of BAX and BAK levels in *RAB25*-overexpressing A2780 cells (Fig. 2f), supporting the potential involvement of *BCL2* family members in regulating *RAB25* action. Thus dependent on the genetic background of the cell, either BAX and BAK, or both (or potentially other apoptotic regulators), were decreased in *RAB25*-transfected cells.

The PI3K pathway, in particular AKT, has been implicated in cell survival[26,27], at least in part, through altered expression of *BCL2* family members[28]. Western blotting analysis showed higher levels of AKT phosphorylation, an indication of activation of the PI3K-AKT pathway, in A2780, HEY, T29 and T80 cells overexpressing *RAB25* (Fig. 2g). Similarly, *RAB25* knock-down by RNAi decreased AKT phosphorylation (Fig. 2h), confirming an interaction between *RAB25* and the PI3K pathway. Thus overexpression of *RAB25* increases signaling through the PI3K pathway and decreases expression of the

Table 1 Increase in cell proliferation by *RAB25* expression

	1% FBS		10% FBS	
Cell lines	pcDNA	*RAB25*	pcDNA	*RAB25*
A2780	37.5 ± 3.5	63.5 ± 7.8	100.5 ± 7.5	145 ± 6.2
OCC1	57 ± 6.3	82.5 ± 4.6	122.5 ± 9.8	181 ± 8.9
SKOV3	58.5 ± 7.2	96.5 ± 6.2	78.5 ± 9.2	128 ± 8.3
T80	95 ± 4.6	154.5 ± 6.8	171 ± 7.4	226 ± 9.3
HEY	119 ± 7.4	225 ± 5.7	348 ± 12.3	538 ± 28.9
MCF-7	60 ± 4.2	109 ± 10.5	142 ± 6.4	174 ± 4.4

Cell counts were performed on day 8 in stable cells lines. Numbers represent cell number × 10,000 cells/ml. Each sample is presented ± s.e.m. of three replicates from one of three representative experiments. Results were confirmed with multiple subclones of each cell line.

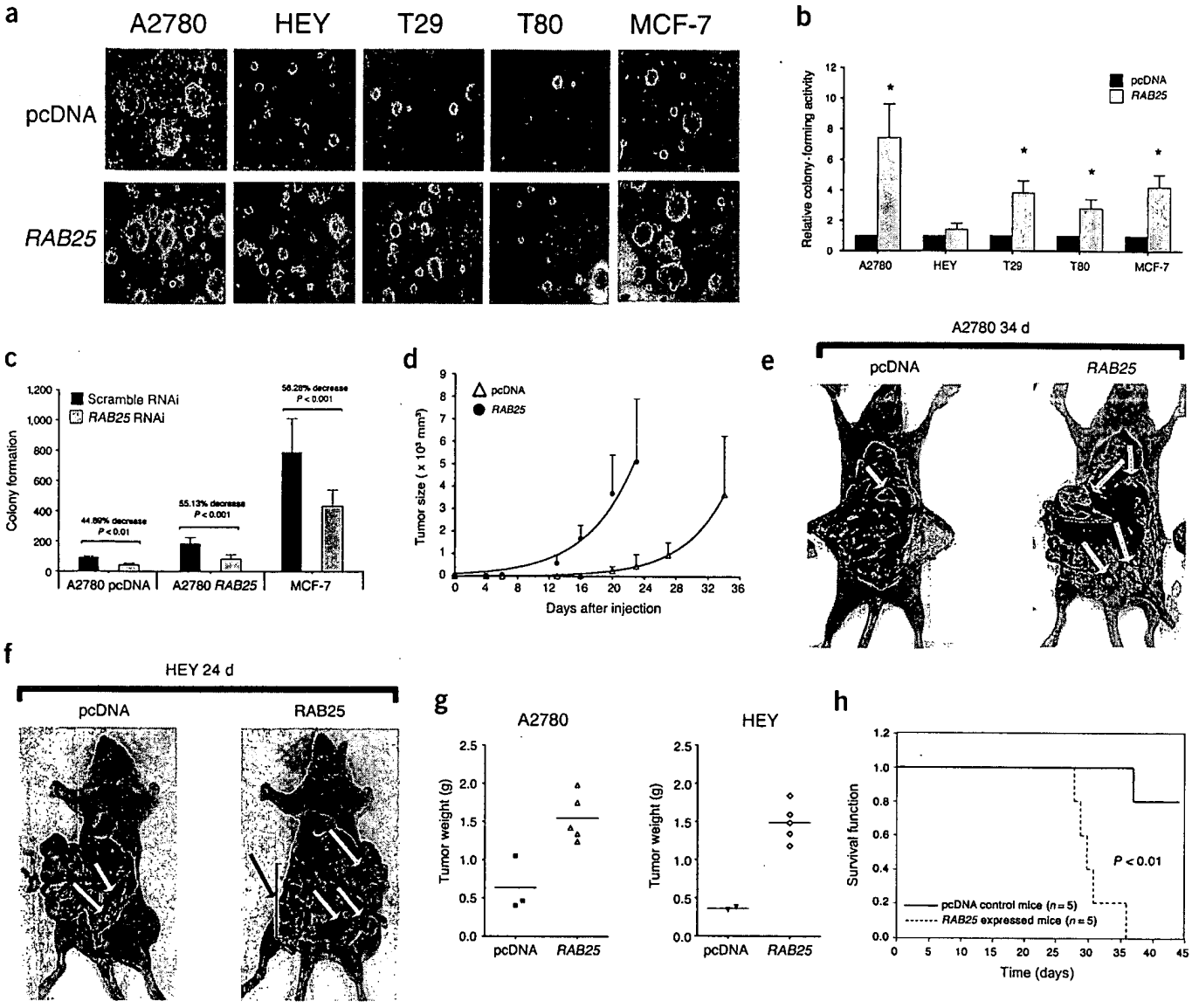

Figure 3 *RAB25* regulates tumorigenicity. Effect of stable *RAB25* (**a**,**b**) and RNAi (**c**) expression on anchorage-independent colony formation. The number of colonies (≥3 mm in diameter) per 10,000 cells plated in pcDNA-transfected cells was 130 ± 32 for A2780, 290 ± 46 for HEY, 68 ± 12 for T29, 28 ± 5 for T80 and 2034 ± 128 for MCF-7. (**d**) Effect of stable *RAB25* expression on subcutaneous growth of A2780 in nude mice. (**e**–**h**) Effect of stable *RAB25* expression on orthotopic intraperitoneal tumor growth (**e**,**f**), weight (**g**) and (**h**) survival (survival curve is from the results of **g**). All stable *RAB25*-transfected cell injections formed tumors, whereas only two and three pcDNA-transfected HEY and A2780 injections formed tumors, respectively). Results are mean ± s.d. from one representative experiment of three performed except mouse studies, which are from one of two experiments.

proapoptotic *BCL2* family members, which likely contributes to resistance to apoptotic stimuli. Although the mechanism by which *RAB25* alters AKT signaling and *BCL2* family expression remains to be fully elucidated, the recent demonstration that multiple signaling molecules, including AKT and small GTPases, associate in a complex on endocytic vesicles[29] provides a potentially unifying mechanism linking AKT with *RAB25*, and subsequent altered cell survival.

The ability of *RAB25* overexpression to block anoikis suggested that *RAB25* may increase the ability of cells to undergo anchorage-independent growth, an *in vitro* surrogate for *in vivo* tumor growth. Indeed, overexpression of *RAB25* markedly increased the number of colonies under anchorage-independent conditions in A2780, T29 and T80 ovarian cells (Fig. 3a,b). Although *RAB25* did not increase colony numbers with HEY cells (Fig. 3b), it did increase the size of HEY cell colonies (Fig. 3a). Similarly, overexpression of *RAB25* in MCF-7 breast cancer cells increased colony-forming activity (Fig. 3a,b). Compatible with a role for *RAB25* in survival under anchorage-independent conditions, a significant decrease in colony-forming activity was observed in *RAB25* RNAi-transfected cells (Fig. 3c, $P < 0.01$). Thus overexpression of RAB25 is sufficient to increase anchorage-independent growth in ovarian and breast epithelial cells.

The marked effects of *RAB25* on cell proliferation, anchorage-independent growth and cell survival suggested that *RAB25* might alter tumor growth *in vivo*. 100% of nude mice injected with *RAB25*-transfected cells developed subcutaneous tumors as compared to only 50% and 70% mice injected with vector transfected A2780 and HEY cells, respectively. Moreover, mice injected with *RAB25*-transfected A2780 and HEY cells developed larger tumors in a shorter time than

mice receiving vector transfected cells (Fig. 3d). *RAB25* overexpression also increased orthotopic intraperitoneal tumor growth (Fig. 3e–g). Further intraperitoneal injection of A2780 cells expressing *RAB25* resulted in rapid tumor accumulation and death compared with empty vector–expressing cells ($P < 0.01$, Fig. 3h). *RAB25* expressing T29 and T80 immortalized ovarian epithelial cells did not grow either subcutaneously or intraperitoneally in nude mice, indicating that *RAB25* is not sufficient to transform ovarian epithelial cells. Rather, *RAB25* increased rates of tumor growth and aggressiveness in already transformed lines. Our data strongly implicate *RAB25* in the aggressiveness of ovarian and breast carcinomas suggesting that *RAB25* could be used to predict patient outcome and may provide a novel therapeutic target. These studies also implicate *RAB25* and, by extension, the RAB GTPase family in tumor aggressiveness. This adds the genes encoding the RAB family to other members of the *RAS* oncogene superfamily as tumorigenic mediators.

METHODS

Patient samples. All patient samples and information were collected under Institutional Review Board–approved (LAB01-144) and HIPAA-compliant protocols at the MD Anderson Cancer Center. All patient samples contained ≥80% tumor on histologic inspection. We obtained NOE by directly scraping ovarian epithelial cells in the operating room into *RNA*later (Ambion). Analysis of the approach indicates that at least 90% of cells are of epithelial origin.

RNA isolation and real-time quantitative PCR. We isolated total RNA from normal ovarian surface epithelial cell preparations directly from the patient, and benign ovarian tumors and advanced (Stages III and IV) ovarian serous epithelial carcinomas by Trizol (Invitrogen) according to the manufacturer's protocol. Fluorogenic Taqman probes were designed based on sequences in GenBank. We determined mRNA levels for the genes of interest by Taqman real-time reverse transcription-PCR using the ABI PRISM 7700 Sequence Detection System (Applied Biosystems) through 40 cycles. We used β-actin as a reference.

Cell lines and transfection. We maintained ovarian caner cell lines in RPMI 1640 containing 10% FBS, and immortalized ovarian surface epithelial cells T29 and T80 in MCDB105:M199 (50:50) containing 10% FBS. We constructed a hemagglutinin-tagged *RAB25* expression vector by PCR amplification and confirmed it by sequencing. Stable *RAB25*-expressing clones were generated by transfection with hemagglutinin epitope–tagged *RAB25* constructs using FuGene 6 (Roche) and selected in G418 for 4 weeks by limiting dilution. We generated at least three clones for each cell line. We performed all experiments with multiple subclones in each cell line and results are representative of several subclones.

RNA interference. We purchased *RAB25*-specific siRNA (5′-GGAGCUCUAUGACCAUGCU-3′) from Xenigon and a scramble RNAi negative control from Ambion. We carried out RNAi transfection in solution T using a Nucleofector according to the manufacturer's protocol (catalog # 4611, Amaxa Biosystem).

Immunoblotting. We cultured cancer cell lines stably expressing *RAB25* in the absence of serum for at least 24 h before protein isolation. We used pcDNA-transfected cells as a control. The proteins were separated by SDS-PAGE and detected with anti-hemagglutinin (1;1000; Covance), anti-bak (1:1000), anti-BAX (1;1000), anti-phospho-AKT (1:1000 dilution, Ser473 or Thr308) or anti-AKT (1:1000 dilution) antibodies (Cell Signaling). We washed the membranes extensively, visualized the proteins by ECL (Amersham Biosciences) and quantified them using NIH image Version 1.61.

Cell proliferation and clonogenic assay. We plated cells stably expressing *RAB25* at a density of 1×10^5 cells/35-mm dish. Cells were then cultured in the presence of 1% or 10% FBS for 8 d. We harvested and counted total cells. We used pcDNA-transfected cells as a control. For anchorage-dependent colony formation, cells were transfected with either pcDNA 3.0 or *RAB25* expression vector. We trypsinized cells 48 h after transfection and replated them in 6 well/plates for 14 d in the presence of G418. Cells were stained with 0.1% Coomassie blue (Bio-Rad) in 30% methanol and 10% acetic acid. We counted the number of colonies formed and expressed the number as fold increase compared with pcDNA-transfected cells. To test the effect of *RAB25* expression on anchorage-independent colony formation, we suspended cells stably expressing pcDNA or *RAB25* at a density of 1×10^4 cells/ml in 1 ml of 0.3% agar dissolved in complete medium containing 25% FBS. Cells were plated in 35-mm dishes precoated with 1 ml of 0.6% agar base. We measured colony-forming efficiency 14–18 d after plating (≥50 cells/colony) and expressed the number as a fold increase related to control vector–transfected cells. All experiments with transfected cells were from multiple individual subclones.

Apoptosis assays. We measured apoptotic cells using paraformaldehyde-fixed cells with an APO-BrdU kit (Phoenix Flow Systems) with flow cytometry. In each experiment, we collected both floating and attached cells and washed them with PBS. We induced apoptosis by culturing cells in 0.1% serum for 48 h, with UV radiation (A2780: 300×100 μJ/cm^3; HEY 150×100 μJ/cm^3; IOSE: 50×100 μJ/cm^3) or paclitaxel (A2780: 200 ng/ml; HEY, T29 and T80: 50 ng/ml). For anoikis assays, we incubated cells on a rocker platform to prevent adhesion for 48 h.

Tumorigenicity in nude mice. To assess the impact of *RAB25* overexpression on tumorigenicity, BALB/c-nu/nu mice (female, 4 weeks old) were injected subcutaneously (above the left hind leg) or intraperitoneally with 5×10^6 *RAB25* overexpressing or control cells. We measured subcutaneous tumors with a digital caliper and killed the mice in compliance with MD Anderson Animal Care and Use Form (ACUF) rules. Intraperitoneal tumor mass was measured by dissection of tumor from the peritoneal cavity and weighing. We performed all animal protocols under an Association for Assessment and Accreditation of Laboratory Animal Care (AALAC)–approved protocol.

Statistical analysis. We statistically evaluated experimental results using the ANOVA test, simple *t*-test, or two-sided log-rank statistical test. Differences were considered significant if $P <_{\wedge} 0.05$. Patients with no further follow-up information are represented by a vertical tick at last point of contact and are weighted in the Kaplan-Meier analysis.

URL. Human Genome Sequencing Consortium assembly http://genome.ucsc.edu/cgi-bin/hgGateway
Gene Expression Omnibus http://www.ncbi.hlm.nih.gov/geo/
Stanford Microarray Database http://genome-www5.stanford.edu/
Ovarian cancer data set[17] http://genome-www.stanford.edy/ovarian_cancer
Breast cancer microarray data set[19] http://genome.www.stanford.edu/breast_cancer/robustness/data.shtml

Note: Supplementary information is available on the Nature Medicine website.

ACKNOWLEDGMENTS
KWC was supported by the Odyssey Program of the Houston Endowment Scientific Achievement award from MD Anderson Cancer Center. We thank N. E. Atkinson's group for help and advice in statistical analysis. We thank R. Lapushin and H. Hall for their support. We thank R. Trost for obtaining patient follow up. We thank the staffs from the MD Anderson Cancer Center and University of California San Francisco ovarian tumor bank for providing ovarian carcinomas. This work is supported by National Institutes of Health SPORE (P50-CA83639) and PPG-PO1 CA64602 to GBM and JWG and P30 grant CA16672-28.

COMPETING INTERESTS STATEMENT
The authors declare that they have no competing financial interests.

Received 7 July; accepted 31 August 2004
Published online at http://www.nature.com/naturemedicine/

1. Pinkel, D. *et al.* High resolution analysis of DNA copy number variation using comparative genomic hybridization to microarrays. *Nat. Genet.* **20**, 207–211 (1998).
2. Goldenring, J.R., Shen, K.R., Vaughan, H.D. & Modlin, I.M. Identification of a small GTP-binding protein, Rab25, expressed in the gastrointestinal mucosa, kidney, and lung. *J. Biol. Chem.* **268**, 18419–18422 (1993).
3. Wang, X., Kumar, R., Navarre. J., Casanova, J.E. & Goldenring, J.R. Regulation of vesicle trafficking in Madin-Darby canine kidney cells by Rab11a and Rab25. *J. Biol. Chem.* **275**, 29138–29146 (2000).
4. Shayesteh, L. *et al.* PI3KCA is implicated as an oncogene in ovarian cancer. *Nat.*

Genet. **21**, 99–102 (1999).
5. Fukushi, Y., Sato, S., Yokoyama, Y., Kudo, K., Maruyama, H., & Saito, Y. Detection of numerical aberrations in chromosome 17 and c-erbB2 gene amplification in epithelial ovarian cancer using recently established dual color FISH. *Eur. J. Gynecol. Oncol.* **22**, 23–25 (2001).
6. Berchuck, A. & Carney, M. Human ovarian cancer of the surface epithelium. *Biochem. Pharmacol.* **54**, 541–544 (1997).
7. Anand, N. *et al.* Protein elongation factor EEF1A2 is a putative oncogene in ovarian cancer. *Nat. Genet.* **31**, 301–305 (2002).
8. Cheng, J.Q. *et al.* AKT2, a putative oncogene encoding a member of a subfamily of protein-serine/threonine kinases, is amplified in human ovarian carcinomas. *Proc. Natl. Acad. Sci. USA* **89**, 9267–9271 (1992).
9. Anzick, S.L. *et al.* AIB1, a steroid receptor co-activator amplified in breast and ovarian cancer. *Science* **277**, 965–967 (1997).
10. Suzuki, S. *et al.* An approach to analysis of large-scale correlations between genome changes and clinical endpoints in ovarian cancer. *Cancer Res.* **60**, 5382–5385 (2000).
11. Patael-Karasik, Y. *et al.* Comparative genomic hybridization in inherited and sporadic ovarian tumors in Israel. *Cancer Genet. Cytogenet.* **121**, 26–32 (2000).
12. Kiechle, M., Jacobsen, A., Schwarz-Boeger, U., Hedderich, J., Pfisterer, J. & Arnold, N. Comparative genomic hybridization detects genetic inbalance in primary ovarian carcinomas as correlated with grade of differentiation. *Cancer* **91**, 534–540 (2001).
13. Zudaire, I. *et al.* Genomic imbalances detected by comparative genomic hybridization are prognostic markers in invasive ductal breast carcinomas. *Histopathology* **40**, 547–555 (2002).
14. Lu, Y.J., Hing, S., Williams, R., Pinkerton, R., Shipley, J. & Pritchard-Jones, K. UK Children's Cancer Study Group Wilms' tumor group. Chromosome 1q expression profiling and relapse in Wilms' tumour. *Lancet* **9330**, 385–386 (2002).
15. Lu, K.H. *et al.* Selection of potential markers for epithelial ovarian cancer with gene expression arrays and recursive descent partition analysis. *Clin. Cancer Res.* **10**, 3291–3300 (2004).
16. Schaner, M.E. *et al.* Gene expression patterns in ovarian carcinomas. *Mol. Biol. Cell.* **14**, 4376–4386 (2003).
17. Sorlie, T. *et al.* Repeated observation of breast tumor subtypes in independent gene expression data sets. *Proc. Natl. Acad. Sci. USA* **100**, 8418–8423 (2003).
18. Calvo, A. *et al.* Alterations in gene expression profiles during prostate cancer progression: functional correlations to tumorigenicity and down-regulation of selenoprotein-P in mouse and human tumors. *Cancer Res.* **62**, 5325–5335 (2002).
19. Mor, O. *et al.* Molecular analysis of transitional cell carcinoma using cDNA microarray. *Oncogene* **22**, 7702–7710 (2003).
20. Wang, W. *et al.* Single cell behavior in metastatic primary mammary tumors correlated with gene expression patterns revealed by molecular profiling. *Cancer Res.* **62**, 6278–6288(2002).
21. Liu, J. *et al.* A genetically defined model for human ovarian cancer. *Cancer Res.* **64**, 1655–1663 (2004)
22. Milhavet, O., Gary, D.S. & Mattson, M.P. RNA interference in biology and medicine. *Pharmacol. Rev.* **55**, 629–648 (2003).
23. Gross, A., McDonnell, J.M. & Korsmeyer, S.J. BCL-2 family members and the mitochondria in apoptosis. *Genes Dev.* **13**, 1899–1911 (1999).
24. Wei, M. *et al.* Proapoptotic BAX and BAK: A requisite gateway to mitochondrial dysfunction and death. *Science* **292**, 727–730 (2001).
25. Degenhardt, K., Chen, G., Lindsten, T. & White, E. BAX and BAK mediate p53-independent suppression of tumorigenesis. *Cancer Cell* **2**, 193–203 (2002).
26. Lu, Y. *et al.* The PTEN/MMAC1/TEP tumor suppressor gene decreases cell growth and induces apoptosis and anoikis in breast cancer cells. *Oncogene* **18**, 7034–7045 (1999).
27. Mills, G.B. *et al.* Role of abnormalities of PTEN and the phosphatidylinositol 3′ kinase pathway in breast and ovarian tumorigenesis, prognosis and therapy. *Semin. Oncol.* **28**, S125–S141 (2001).
28. Kennedy, S.G. *et al.* The PI 3-kinase/Akt signaling pathway delivers an anti-apoptotic signal. *Genes Dev.* **11**, 701–713 (1997).
29. Delcroix, J.D., Valletta, J.S., Wu, C., Hunt, S.J., Kowal, A.S. & Mobley, W.C. NGF signaling in sensory neurons: evidence that early endosomes carry NGF retrograde signals. *Neuron* **39**, 69–84 (2003).